Early treatment with C1 esterase inhibitor improves weight but not memory deficits in a rat model of status epilepticus

Nicole D. Schartz[1], **Alexandra L. Sommer**[1], **Samantha A. Colin**[1], **Loyda B. Mendez**[2], **Amy L. Brewster**[*,1,3,4]

[1]Department of Psychological Sciences, Purdue University, West Lafayette, IN 47907

[2]School of Science & Technology, Ana G. Mendez University, Carolina, PR 00984

[3]Purdue Institute for Integrative Neuroscience, Purdue University, West Lafayette, IN 47907

[4]Weldon School of Biomedical Engineering, Purdue University, West Lafayette, IN 47907

Abstract

Background: Status epilepticus (SE) is a prolonged and continuous seizure that lasts for at least 5 minutes. An episode of SE in a healthy system can lead to the development of spontaneous seizures and cognitive deficits which may be accompanied by hippocampal injury and microgliosis. Although the direct mechanisms underlying the SE-induced pathophysiology remain unknown, a candidate mechanism is hyperactivation of the classical complement pathway (C1q-C3 signaling). We recently reported that SE triggers an increase in C1q-C3 signaling in the hippocampus that closely paralleled cognitive decline. Thus, we hypothesized that blocking activation of the classical complement pathway immediately after SE may prevent the development of SE-induced hippocampal-dependent learning and memory deficits.

Methods: Because C1 esterase inhibitor (C1-INH) negatively regulates activation of the classical complement pathway, we used this drug to test our hypothesis. Two groups of male rats were subjected to 1 hr of SE with pilocarpine (280-300 mg/kg, i.p.), and treated with either C1-INH (SE +C1-INH, 20 U/kg, s.c.) or vehicle (SE+veh) at 4, 24, and 48 hours after SE. Control rats were treated with saline. Body weight was recorded up to 23 days after SE. At this time, recognition and spatial memory were determined using novel object recognition (NOR) and Barnes maze (BM), respectively, as well as locomotion and anxiety-like behaviors using open field (OF). Histological

[*]**Corresponding Author:** Amy L. Brewster, Ph.D., Department of Psychological Sciences, College of Health and Human Sciences, Purdue University, 703 Third Street, West Lafayette, IN, 47907, # Tel: (765) 494-5075; # Fax: (765) 496-2670, abrewst@purdue.edu.

Authors' Contributions: NDS designed research, performed research, analyzed data, wrote the paper; ALS performed research and analyzed data; SAC performed research; LBM performed research, analyzed data; ALB designed research, analyzed data, wrote the paper.

Ethics approval and consent to participate: *Ethics approval*, all animal procedures were approved by the Purdue Animal Care and Use Committee (Protocol #1309000927); *consent to participate:* Not applicable.

Consent of Publication: Not applicable

Availability of data and materials: Please contact corresponding author for data requests

Competing interests: The authors declare no competing financial interests.

and biochemical methods were used to measure hippocampal injury including cell death, microgliosis, and inflammation.

Results: One day after SE, both SE groups had a significant loss of body weight compared to controls (p<0.05). By day 14, the weight of SE+C1-INH rats was significantly higher than SE+veh rats (p<0.05), and was not different from controls (p>0.05). At 14 days post-SE, SE+C1-INH rats displayed higher mobility (distance travelled and average speed, p<0.05) and had reduced anxiety-like behaviors (outer duration, p<0.05) than control or SE+veh rats. In NOR, control rats spent significantly more time exploring the novel object vs. the familiar (p<0.05), while rats in both SE groups spent similar amount of time exploring both objects. During days 1–4 of BM training, the escape latency of the control group significantly decreased over time (p<0.05), whereas that of the SE groups did not improve (p>0.05). Compared to vehicle-treated SE rats, SE+C1-INH rats had increased levels of C3 and microglia in the hippocampus, but lower levels of caspase-3 and synaptic markers.

Conclusions: These findings suggest that acute treatment with C1-INH after SE may have some protective, albeit limited, effects on the physiological recovery of rats' weight and some anxiolytic effects, but does not attenuate SE-induced deficits in hippocampal-dependent learning and memory. Reduced levels of caspase-3 suggest that treatment with C1-INH may protect against cell death, perhaps by regulating inflammatory pathways and promoting phagocytic/clearance pathways.

Introduction

Epilepsy is a neurological disorder that affects over 70 million people world-wide [1] and is characterized by spontaneous seizures driven by an excitatory/inhibitory imbalance in the brain [2]. Epilepsy is highly comorbid with other neurological conditions including developmental disorders such as autism spectrum disorder, psychiatric problems such as anxiety and depression, and cognitive disruptions such as learning and memory deficits [3–5]. The pathophysiology of epilepsy can be exacerbated by prolonged and continuous seizures (lasting 5 mins), also known as status epilepticus (SE) [6]. Episodes of SE can occur in individuals with epilepsy as well as following adverse events such as traumatic brain injury (TBI), stroke, alcohol withdrawal, or brain tumors in non-epileptic people [6]. SE increases the risk of subsequently developing epilepsy to 66.7% [7]. Temporal lobe epilepsy (TLE) is a common form of SE-triggered epilepsy that is highly comorbid with cognitive impairments [8]. In fact, the most common concern of epilepsy patients behind unexpected seizures is memory problems [9], in particular deficits in long-term memory [10]. Extensive evidence from animal models support that a single episode of SE results in deficits in recognition and hippocampal-dependent spatial memory [11–15]. Because the mechanisms underlying cognitive decline after SE are still not defined, our research objective is to identify novel therapeutic targets to prevent or attenuate the SE-induced

cognitive comorbidities. In this study we focused on the immune classical complement pathway as a candidate mechanism.

The classical complement pathway is part of the innate immune system and acts as a first responder to injury or infection [16, 17]. Complement activation aids in tagging and clearing bacteria, dead cells, and cellular debris. Activation of the classical complement pathway occurs when the recognition protein, C1q, associates with C1r and C1s to form the C1 complex which initiates the downstream activation and cleavage of C3 into C3a and C3b fragments to regulate inflammatory (C3a) and phagocytic (C3b) mechanisms [18]. Under physiological conditions C1q-C3 signaling is essential for the proper development and maintenance of neuronal connectivity and function [19–21]. In contrast, C1q-C3 hyperactivation is associated with aberrant neuronal circuitries as well as cognitive deficits in rodent models of Alzheimer's disease (AD) [22], TBI [23], and ischemia [24]. In these contexts inhibition of complement C1q or C3 signaling results in protection against deficits in hippocampal-dependent spatial memory [23], contextual learning [25], and cognitive flexibility [25]. Recently, we reported increased protein levels of complements C1q and iC3b in brain samples of human drug-resistant epilepsy [26] and in rat model of SE and acquired TLE [27]. Specifically, we found that a single episode of SE provoked long-lasting increases of C1q and iC3b protein levels the hippocampus that paralleled the development of spatial learning and memory deficits and higher seizure frequency [27]. Taken together these data suggest that hyperactivation of the classical complement pathway in the brain may promote cognitive decline, and suggest a role of C1q-C3 signaling in SE-induced learning and memory deficits.

The classical complement pathway is negatively regulated by the C1 esterase inhibitor (C1-INH) which inhibits the formation of the C1 complex thereby reducing C1q-mediated activation of C3 [28]. In rodent models of TBI and ischemia/stroke acute C1-INH treatment reduces the neurological and cognitive pathophysiology that is associated with brain injury [23, 29, 30]. Thus, we hypothesized that early treatment with C1-INH immediately after SE may attenuate hippocampal injury and hippocampal-dependent spatial learning and memory deficits that are associated with SE and acquired TLE. In this study, we administered C1-INH to a group of rats that underwent SE and compared them to vehicle-treated SE rats and sham-treated controls with a battery of behavioral tests to determine hippocampal-dependent learning and memory function. In addition, throughout the study we recorded the animals' weights, determined locomotion and anxiety-like behaviors, and evaluated the impact of C1-INH treatment on SE-induced hippocampal microgliosis, inflammation, cell death, and synaptic loss.

Materials and Methods

Animals.

Male Sprague Dawley rats (150-175 grams) (Envigo Laboratories, Indianapolis, IN) were housed in the Psychological Sciences Building at Purdue University. Rats were housed in pairs with ambient temperature maintained at 22°C, and a 12-hour (hr) light/dark cycle (8:00 to 20:00 hr light). All animals had free access to food and water (24hr/7days). All animal

procedures were performed in accordance to the approved NIH and Institutional guidelines and the Purdue Animal Care and Use Committee (Protocol #1309000927).

Pilocarpine-induced status epilepticus.

SE was induced using a previously described protocol [27, 31]. Rats were injected with scopolamine methylbromide (1 mg/kg) intraperitoneally (i.p.) 30 minutes prior to injections of 0.9% saline (sham control group) or pilocarpine (280-300 mg/kg; i.p.; Sigma-Aldrich, St Louis, MO) (SE group). Class 4.5 limbic motor seizures or higher on the Racine scale [32] indicated SE. SE was stopped after 1 hour with diazepam (10 mg/kg; i.p.; Hospira, Inc., Lake Forest, IL). I.P. injections of 0.9% saline (AddiPak) were administered two hours after SE and as needed. Rat chow was supplemented with sliced peeled apples, Kellogg's Fruit Loop cereal, and/or chocolate Ensure for up to one week after SE. Immediately after SE, rats typically lose about 10% of their body weight, and treatment with immunomodulatory drugs can accelerate weight recovery [33]. Therefore, we recorded body weight daily for the first two weeks after SE. In total, 64 rats were injected with pilocarpine and 22 with saline (controls). Of the rats that received pilocarpine, 2 died during or shortly after SE and 13 failed to reach SE (stage 5-6). Rats that reached SE and survived (48 rats) were randomly assigned to C1-INH (18 rats) or vehicle (30 rats) treatment groups. Rats were used for behavior (52 rats), western blots (24 rats), immunohistochemistry (10 rats), and *Solid-based immunoassay* (6 rats), with rats being used for multiple tests when possible.

C1-INH treatment.

Rats were given C1-INH (EMD Medicals Inc., San Diego, CA) (20 U/kg) at 2, 24, and 48 hours after SE via subcutaneous (s.c.) injection. SE rats were randomly selected to receive C1-INH (SE+C1-INH) injections or vehicle (SE+veh) injections (0.9% saline). Control rats were given vehicle.

Open Field (OF).

At the start of each behavior day, all animals were placed in individual holding cages in a central suite adjacent to the testing room and allowed to acclimate in the dark for 30-60 minutes. Acclimation began each day at approximately 9:00am, one hour after the light phase began, to avoid disruption of the circadian cycle. For OF, rats were placed in an open arena (62 X 62 X 46 cm) at 3 and 14 days after pilocarpine or sham treatments. Rats were allowed to explore the arena for 20 minutes under red light conditions, and were video recorded from above. The Any-Maze video tracking system V4.99 (Wood Dale, IL) was used to determine distance travelled and average speed as measures of locomotion, and freezing and time spent along the outer part of the arena (outer duration) as measures of anxiety-like behaviors [34].

Novel Object Recognition (NOR) test.

The NOR test was used to assess recognition memory as previously described [21]. Fifteen days after SE, rats were placed in the OF test chamber for 5 minutes and allowed to explore two similar objects (trial 1). Two hours after trial 1, one of the objects was replaced by a novel object. Then rats were placed back in the testing chamber and were allowed to explore

the objects for 5 minutes (trial 2). The placement of the novel and familiar objects was counterbalanced to control for any potential side preferences. All trials were conducted under red light conditions and the arena and objects were thoroughly cleaned with 70% ethanol between trials. Exploration time was defined by the rats' noses coming within 1 cm of the objects, which was tracked with Any-Maze video tracking system and verified with hand scoring by investigators blinded to treatment groups. Percent of time spent exploring the left versus right (trial 1) or familiar versus novel (trial 2) was compared. Recognition of the familiar object (Recognition Index; RI) was determined by subtracting the time spent with the familiar object during trial 2 (F2) from the time spent with the corresponding object (left or right) in trial 1 (F1) as a proportion of total exploration time $[(F1-F2)/(F1+F2)]$ [27]. Discrimination of novel and familiar objects during trial 2 (Discrimination Index; DI) was determined by subtracting the time spent with the familiar object (F) from the time spent with the novel object (N) $[(N-F)/(N+F)]$ as a proportion of total exploration time during trial 2 [35].

Barnes Maze (BM).

Two days after NOR, rats were tested for hippocampal-dependent spatial learning and memory with BM using our previously described protocol [27]. The testing arena consisted of a black circular platform (1.22 m diameter and elevated 1.68 m) with 18 equally spaced holes (10.16 cm diameter) along the outer edges, one with a removable escape box placed underneath. Visual cues for navigation were placed on all walls. Acclimation occurred in the dark to exacerbate the anxiogenic effects of bright lights during BM testing, in order to promote exploration of the maze to find and enter the escape box. Rats were habituated to the escape box on day 17 (See Figure 1A). On BM training days 1-4, rats were placed inside an opaque start box located in the center of the BM platform. After a 10-second delay, bright lights were turned on and the start box was lifted. Rats had up to 3 minutes to find and enter the escape box, or were guided to it after this time terminated. Rats were allowed to remain in the box for 1 minute. This was repeated four times each day, separated by 15-20 minutes. Latency to enter the escape box was recorded. On BM day 5, a probe trial (PT) was performed. All holes, including target hole, on the BM platform were covered to test time spent on top of the target hole (location of escape box). Rats were allowed 90 seconds on the platform during the PT. The BM platform was thoroughly cleaned with 70% ethanol and rotated between each trial, with the escape box remaining in the same spatial location. To create a single index that could describe spatial learning acquisition for each rat at the end of BM training, we subtracted the latency to reach the escape hole on day 4 from the latency on day 1. In a normally behaving rat, the latency would be shorter on day 4 compared to day 1, which would result in a positive number. If a rat did not learn, the index would be close to zero, and if a rat took longer to escape at the end of training, the number would be negative. This index controls for any potential variation in initial latency (although we did not observe a significant difference in day 1 escape latency in any group) [27].

Immunohistochemistry (IHC).

All C1-INH-treated tissue samples in this study were processed concurrently with a subset of the samples from both SE and control groups which were included in our published study Schartz et al., 2016 [31]. Therefore, all IHC and densitometry analysis were done exactly as

previously described [31]. Briefly, brains were perfused with ice cold 1X phosphate buffered saline (PBS; 137 mM NaCl, 2.7 mM KCl, 4.3 mM Na$_2$HPO$_4$, 1.47 KH$_2$PO$_4$, pH 7.4), then fixed by transcardiac perfusions with 4% paraformaldehyde. They were removed, post-fixed, cryoprotected (30% sucrose), sliced (coronal, 50 μm), and immunostained using anti-rabbit IBA1 (1:500; Wako Chemicals Cat# 019-19741, RRID: AB_839504) and anti-rabbit cleaved caspase 3 (1:1K; Cell Signaling Technology Cat# 9661, RRID: AB_2341188). Biotinylated goat anti-rabbit secondary antibodies (1:2000; Vector Laboratories Cat# BA-1000 RRID:AB_2313606) were used along with ABC Avidin/Biotin complex solution and DAB Peroxidase (HRP) Substrate Kit, 3,3'-diaminobenzidine (Vector Laboratories) to develop and visualize the immunostaining. Four to six sections between the Bregma coordinates −3.00mm and −5.28mm were processed per brain. Densitometry analysis of IBA1 signal in the hippocampal CA1 region and quantification of caspase-3 positive cells on the CA1 pyramidal cell layer were performed using the ImageJ software V1.49 (NIH; Bethesda, MD).

Western Blotting (WB).

Immunoblotting was performed following protocols described previously [13, 27]. Briefly, following transcardiac perfusions with ice cold 1X PBS, hippocampi were removed, rapidly frozen, and stored at −80°C. Tissue samples were homogenized (100 mM Tris-HCl, pH 7.4, 0.32 M sucrose, 1 mM EDTA, 5 mM Hepes, with 0.2% protease inhibitor cocktail) and protein concentration determined with Bradford Protein Assay (Bio-Rad, Hercules, CA). SDS-PAGE was done with equal amounts of protein diluted in Laemmli buffer (4X: 0.25 M Tris, pH 6.8, 6% SDS, 40% sucrose, 0.04% Bromophenol Blue, 200 mM Dithiothreitol). Samples were transferred to PVDF membranes (GE Healthcare, Chicago, IL) and blocked in 5% non-fat milk diluted in 1X Tris buffered saline (50 mM Tris-HCl, pH 7.4, 150 mM NaCl) with 0.1% Tween (1X TBS-T) for 1 hr at room temperature (RT). Membranes were incubated in the following primary antibodies at 4°C overnight or for 2 hours at room temperature: goat anti-C3 (1:500; MP Biomedical Cat# 0855730, RRID: AB_2334618, Solon, OH), rabbit anti-C3 (1:1k; Abcam Cat# ab200999), mouse anti-PSD95 (1:50k; UC Davis/NIH NeuroMab Facility Cat# 75-028, RRID:AB_2292909), mouse anti-VGat (1:1k; UC Davis/NIH NeuroMab Facility Cat# 73-457, RRID:AB_2629422), mouse anti-VGlut1 (1:1k; UC Davis/NIH NeuroMab Facility Cat# 75-066, RRID:AB_2187693) and rabbit anti-actin (1:5K; Sigma-Aldrich Cat# a2066, RRID: AB_476693). Membranes were then incubated in horseradish peroxidase-labeled secondary antibodies: anti-rabbit IgG (1:5K; Cell Signaling Technology Cat# 2729Sm RRID: AB_1031062, Danvers, MA) or donkey anti-goat IgG (1:5K; Millipore Cat# AP180P RRID: AB_92573, Temecula, CA) for 1-2 hours at room temperature. Membranes were thoroughly washed after both primary and secondary antibodies in 1X TBS-T (3x5 minutes). Following the washes, membranes were incubated with enhanced chemiluminescence prime WB detection reagent (GE Healthcare). Immunoreactive bands were captured on autoradiography film (MIDSCI, St. Louis, MO). Films were developed and scanned for densitometry analysis using Image J software V1.49 (NIH; Bethesda, MD) as described previously [13, 36]. Densitometry of the bands of interest was normalized for loading to the corresponding actin of the same sample.

Solid-based immunoassay:

The concentration of 24 cytokines, chemokines and growth factors were determined with a multiplex magnetic bead-based immunoassay (Bio-Plex Pro™ Rat Cytokine 23-Plex Immunoassay, Bio-Rad, Hercules, CA) using the Luminex MAGPIX® system. Brain homogenates were tested in duplicates. Data were analyzed with the Bio-Plex Manager 6.1 software (Bio-Rad, Hercules, CA) using a 5-parameter logistic curve and normalized against total protein concentration [31].

Statistical Analyses:

Weights were compared using a repeated measures Analysis of Variance (ANOVA). OF was compared using one-way ANOVA. Object exploration during NOR trials 1 and 2 was compared using paired t-tests, and the RI and DI were compared using one-way ANOVA. BM training was compared using a repeated measures ANOVA. BM probe trial and the learning index were compared using a one-way ANOVA. All ANOVAs were followed up using Tukey's post hoc test for multiple comparisons. Because the current study was run in parallel to a subset of control and SE samples which SE-induced changes relative to controls at 3 and 14 days after SE were reported for IBA1, Caspase 3 and C3 in our previous studies [27, 31], here we analyzed data from IHC (Fig. 6A, 6B and 7A), WB (Fig. 6A and 7B), and solid-based immunoassay (Fig. 6D–E) using t-tests between SE and SE+INH groups that were run concurrently. All analyses were performed using GraphPad Prism (V. 8.0.1). Significance level was set at $\alpha = 0.05$. *A priori* power analyses were done using G*Power (V. 3.1.9.2) to determine sample size required to achieve power of 0.8 using data from our previous study [27]. Graphs were made with GraphPad Prism and figures were made in Photoshop (V. 2017 1.1). Statistics were reported in the format suggested by Cole (2015) [37].

Results

Acute treatment with C1-INH after SE accelerates weight gain.

C1-INH is a serpin that competitively binds the serine proteases C1r and S1s, blocking activation of the C1 complex and thus preventing the downstream formation of C3 convertase via the classical pathway [38]. We and others found increased levels of C3 complement molecules in the hippocampus as early as 3 days after SE [27, 39–41] that were associated with neuroinflammation and cognitive decline in rodent models of epilepsy [27, 40]. Because acute treatment with C1-INH attenuated the negative effects of cerebral ischemia and ischemia-reperfusion brain injury in rodents [30, 42, 43], here we investigated the effects of C1-INH on SE pathophysiology and neuropathology. Following SE induction and C1-INH treatment we measured weight and evaluated anxiety-like behaviors, learning, and memory between 3 and 23 days after SE (Figure 1A). To evaluate the effects of C1-INH on the neuropathology of SE we collected fixed brains for histology and fresh hippocampi for immunoassays (WB and solid-based) at both 3 and 14 days after SE from a subset of animals. These time points were selected because they represent the peak of the significant changes in inflammation and apoptosis at 3 days, and microgliosis and synaptodendritic alterations at 14 days [13, 27, 31, 44]. Rats that received pilocarpine and developed SE

(Figure 1B) according to the Racine scale [32] were randomly distributed in two groups for treatment with vehicle or C1-INH.

To monitor the rats' recovery after SE we performed routine daily measurements of their body weight (Figure 1A). We recorded the weight of all rats on days 0-14 and day 23 after SE (end of experiments) (Figure 2). We stopped daily weight monitoring after 14 days because at that point rats were consistently gaining weight and not exhibiting any signs of distress, and to minimize potential stressors during the behavioral testing. All rats consistently gained weight throughout the duration of the experiment (Controls: 7.05 ± 0.39 grams/day (Mean $\pm$ SEM); SE: 5.68 ± 0.93 grams/day; SE+C1-INH: 8.02 ± 0.70 grams/day). There was a significant interaction of treatment group and day $[F_{(30, 537)} = 6.27, p < 0.0001]$ with significant effects for both time $[F_{(2.96, 105.8)} = 536.6, p < 0.0001]$ and treatment $[F_{(2, 41)} = 17.58, p < 0.0001]$. On experimental day 0, prior to pilocarpine or sham injection, rats were randomly assigned to an experimental group and all rats had similar weights (C vs. SE+veh, $p = 0.8$; C vs. SE+C1-INH, $p = 0.8$; SE+veh vs SE+C1-INH, $p > 0.9$). By day 1, SE+veh rats lost 25 ± 6.13 g, SE+C1-INH rats lost 24.60 ± 6.82 g, and controls gained 1.4 ± 6.61 g. From 1 to 23 days after SE the weights of the rats in the SE +veh group remained significantly decreased when compared to the control group ($p < 0.05$). In contrast, the average weight of the rats in the SE+C1-INH group were not different from the controls at 12 ($p = 0.09$), 13 ($p = 0.3$), 14 ($p = 0.1$) and 23 days ($p > 0.9$). By the last day of the experiment, the SE+veh group weighed significantly less than the control ($p = 0.04$) and SE+C1-INH group ($p = 0.03$). Taken together, these data suggest that treatment with C1-INH after SE accelerated weight recovery.

Acute treatment with C1-INH increased locomotion and reduced anxiety-like behaviors two weeks after SE.

We measured measuring locomotion and anxiety-like behaviors in order to detect potential deficits that may influence exploratory behaviors in all control, SE+veh, and SE+C1-INH groups using OF at 3 and 14 days post SE (Figure 3). We determined total distance traveled (Figure 3A and E) and average speed (Figure 3B and F) to assess locomotion, and time spent freezing (Figure 3C and G) and percent of time spent in the outer section of the OF arena (Figure 3D and H) to assess anxiety-like behaviors. At 3 days after SE, there were no significant group differences in distance $[F_{(2, 14)} = 0.14, p > 0.9]$, speed $[F_{(2, 14)} = 0.13, p > 0.9]$, freezing $[F_{(2, 14)} = 0.18, p = 0.8]$, or outer duration $[F_{(2, 14)} = 0.83, p = 0.5]$. At 14 days post SE, we observed significant group effects in distance traveled (Figure 3E, $[F_{(2, 41)} = 5.48, p = 0.008]$) and average speed (Figure 3F, $[F_{(2, 41)} = 5.61, p = 0.007]$). Overall, the control and SE+veh groups were not significantly different from each other in distance ($p > 0.9$) and speed ($p > 0.09$). However, rats from the SE+C1-INH group showed significantly increased distance travelled and average speed compared to control (distance, $p = 0.02$; speed, $p = 0.02$) and SE+veh (distance, $p = 0.01$; speed, $p = 0.01$) groups. While we found no significant group effects on freezing at 14 days (Figure 3G, $[F_{(2, 41)} = 0.09, p > 0.9]$), we found a significant effect on outer duration (Figure 3H, $[F_{(2, 40)} = 5.37, p = 0.009]$), with the SE+C1-INH group spending significantly less time in the periphery of the arena when compared to control ($p = 0.03$) and SE+veh ($p = 0.01$) groups. Altogether, acute treatment with C1-INH had no effect on locomotion and anxiety at 3 days after SE.

However, acute treatment increased locomotion and reduced anxiety-like behaviors at 2 weeks post SE, suggesting an anti-anxiety (anxiolytic) effect of C1-INH treatment.

Acute C1-INH treatment did not affect SE-induced hippocampal-dependent memory deficits.

Deficits in cognitive performance often occur in conjunction with spontaneous recurrent seizures in humans and in rodent models of SE and TLE [45–50]. SE and TLE are highly associated with hippocampal injury and thereby deficits in hippocampal-dependent recognition memory [27, 31, 51]. We previously reported that SE-induced hippocampal complement activation paralleled deficits in recognition and spatial hippocampal-dependent memory [27]. Thus, to determine if acute C1-INH treatment modified these SE-induced outcomes, hippocampal-dependent behaviors were determined in the control, SE+veh, and SE+C1-INH groups using the NOR (Figure 4) and BM (Figure 5) tests. In NOR trial 1, the time spent exploring two similar objects was not significantly different for the control [$t_{(12)}$ = 0.51, p = 0.6], SE+veh [$t_{(15)}$ = 0.17, p > 0.9], or SE+C1-INH [$t_{(12)}$ = 0.61, p = 0.6] groups (Figure 4A). In addition, we measured the total time spent exploring both objects, and found no difference in object exploration between the three treatment groups [$F_{(2, 39)}$ = 0.05, p > 0.9] (data not shown). In NOR trial 2, the control group spent significantly more time exploring the novel object than the familiar object [$t_{(12)}$ = 2.93, p = 0.01] (Figure 4B). In contrast, rats in the SE+veh and SE+C1-INH groups spent a similar amount of time exploring the familiar and the novel objects (SE+veh, [$t_{(15)}$ = 1.37, p = 0.2]; SE+C1-INH, [$t_{(12)}$ = 0.28, p = 0.8]) (Figure 4B) suggesting a deficit in recognition memory. As in trial 1, there was no difference in total object exploration during trial 2 between the groups [$F_{(2, 39)}$ = 0.31, p = 0.7] (data not shown). To compare recognition memory between treatment groups we used indexes for object recognition (Figure 4C) and discrimination (Figure 4D). The RI compares the time spent exploring the familiar object during trial 2 with trial 1 exploration. An RI greater than 1 indicates habituation to the familiar object. There was no group effect on the NOR RI [$F_{(2, 41)}$ = 1.05, p = 0.4]. However, the DI was significantly different between groups [$F_{(2, 41)}$ = 3.31, p = 0.04]. Tukey's post hoc test determined that the DI was significantly lower in the SE+veh group compared to the controls (p = 0.03). These findings support that whereas control rats discriminated between a novel and familiar object, and preferred exploration of the novel object, SE+veh rats did not make that distinction. Furthermore, treatment with C1-INH after SE did not prevent the development of deficits in recognition memory.

Hippocampal-dependent spatial learning and memory was determined using the BM (Figure 5). Rats were trained over 4 days, with 4 trials per day to find a hidden escape box on a flat, circular platform. Latency to reach and enter the escape box was averaged per day (Figure 5A–B). There was a significant effect of treatment on the latency to first reaching the target (Figure 5A) [$F_{(2, 21)}$ = 10.76, p = 0.0006], but no effect of day [$F_{(1.88, 39.40)}$ = 2.71, p = 0.08], and no interaction [$F_{(6, 63)}$ = 0.12, p > 0.9]. We also found a significant effect on latency to enter the escape box (Figure 5B). We found a significant interaction between training day and treatment group [$F_{(6, 63)}$ = 2.50, p = 0.03]. There was a significant effect of treatment on escape latency [$F_{(2, 21)}$ = 10.18, p = 0.0008], but no effect of day [$F_{(2.69, 56.56)}$ = 2.17, p = 0.1]. The escape latency on the first day was similar in all experimental

groups (C vs. SE+veh, $p = 0.7$; C vs. SE+C1-INH, $p = 0.4$; SE+veh vs SE+C1-INH, $p = 0.8$), indicating a consistent baseline. On days 2 and 3 of training, the escape latency was similar in controls and SE+veh rats (day 2, $p = 0.4$; day 3, $p = 0.2$), but it was faster in controls compared to the SE+C1-INH group (day 2, $p = 0.04$; day 3, $p = 0.006$). On the fourth and last day of training, the control group decreased their escape latency to 21.38 seconds from 82.56 seconds on day one, suggesting that control animals learned the location of the escape box. In contrast, both the SE+veh and SE+C1-INH groups had significantly longer escape latencies than the controls on day 4 (C vs. SE+veh, $p = 0.0003$; C vs. SE+C1-INH $p = 0.0005$). On the fifth day of BM, the escape box was covered and rats were allowed to explore the table for 90 seconds (probe test, PT) (Figure 5C–D). There was no significant group effect on time spent on top of the covered escape box [$F(2, 21) = 2.78$, $p = 0.09$]. The results of the BM training were converted into a learning index to highlight the acquisition of learning over time with one value (Figure 5E). A value above 1 indicated that an animal's escape latency was decreased between training day 1 and 4, thus suggesting that learning occurred in this test. We compared the indexes for the control, SE+veh, and SE+C1-INH groups and found a significant effect [$F(2, 21) = 8.23$, $p = 0.002$], with the index being higher for the control group compared to the SE+veh group ($p < 0.05$) or the SE+C1-INH group ($p < 0.01$). Taken together these findings suggest that SE-induced deficits in recognition and spatial memory were not attenuated by C1-INH administered acutely after SE.

Acute C1-INH treatment after SE reduced cell death early after SE, but exacerbated C3bα increases and synaptic protein loss in the hippocampus

Next, we examined brain tissue samples to determine the effects of C1-INH in the neuropathology of SE at 3- (Fig. 6) and 14-days (Fig. 7) after SE. C1-INH is expected to inactivate C1r/C1s proteases in the C1 complex and the MBL complexes of the classical and lectin pathways, respectively [43, 52], and prevent activation of the complement C3 via these pathways [53]. Therefore, we measured the protein levels of the C3 fragment C3bα one day after the last C1-INH injection (Fig. 6A). Because downstream activation of the complement cascade regulates microgliosis and inflammation [53], which are events associated with cell loss early after SE [31], we determined the effects of C1-INH on apoptosis through neuronal caspase 3 activation (Fig.6B), microgliosis using the IBA1 marker (Fig. 6C), and on the levels of 24 different inflammatory molecules in the hippocampus (Fig. 6D–E). Note that C1-INH-treated SE samples from this current study were run concurrently with a subset of control and SE samples included in previous studies for the same outcome measures [27, 31]. We previously reported increases in IBA1 and cleaved-caspase 3 at 3 days after SE [31]. Therefore, here we compared and report t-test analyses for the SE+veh and SE+C1-INH groups. We found that the protein levels of C3bα were not significantly different between the SE+veh and SE+C1-INH at 3 days after SE [$t(4) = 2.313$, $p = 0.08$] suggesting the possibilities that the effects of C1-INH to block C1r/C1s proteases is short-acting, or that a higher dose or prolonged treatment is needed to inhibit C3 activation at 3 days after SE. However, we found that the number of caspase 3 positive cells was significantly reduced in the CA1 pyramidal cell layer of the SE+INH group when compared to the SE+veh group [($t(6) = 3.560$, $p = 0.0119$] (Fig. 6B). This finding paralleled a significant increase in the intensity of IBA1 immunostaining in the CA1 hippocampus of the SE+C1-INH group

relative to the SE+veh group [(t(6) = 3.378, p = 0.0149] (Fig. 6C), that was not associated with altered levels of inflammatory molecules ($p > 0.05$) (Fig. 6D,E). It is possible that the accumulation of non-inflammatory and potentially phagocytic microglia is responsible for the removal of dead/dying cells, and thereby the decreased numbers of apoptotic cells (Fig. 6B), or that C1-INH after SE is neuroprotective.

At two weeks following SE the density of IBA1-stained microglia (Fig. 7A) or levels of 24 inflammatory molecules in the hippocampus were not different between the SE+veh and SE-C1-INH groups (data not shown). Using an antibody specific for C3bα we confirmed significant increases in the levels of C3 activation in hippocampi of SE rats compared to controls (p = 0.0026). Interestingly, C3bα levels were elevated in the SE+C1-INH group relative to the SE group (p = 0.03). Because C3 is linked to microglial-mediated synaptic elimination [17, 19, 22, 25, 54] we determined the effects of C1-INH in the levels of the synaptic proteins PSD95, VGlut, and VGat (Fig. 7B–D). At two weeks after SE, there were significant differences in levels of PSD95 [F(2, 6) = 0.4335, p = 0.001], VGat [F(2, 6) = 1.696, p = 0.002], and VGlut [F(2, 6) = 1.139, p = 0.0002]. Protein levels of VGat and VGlut were significantly decreased in the SE group compared to controls (VGat, p = 0.0317; VGlut, p = 0.0004) while PSD95 was not different between these groups (p = 0.1354). Unexpectedly, we also observed that this SE-induced loss of synaptic proteins was more robust in SE+C1-INH group compared to the SE group (PSD95, p = 0.0019; VGat, p = 0.0120; VGlut, p = 0.04). Linear regression analyses showed a significant correlation between high C3bα protein levels and low levels of PSD95 (r^2 = 0.6969, p = 0.0027), VGat (r^2 = 0.8851, p = <0.0001), and VGlut (r^2 = 0.8581, p = 0.0003) within the same samples. Taken together these data suggest that C1-INH given immediately after an episode of SE can have short-term protective effects but also had long-lasting effects in exacerbating C3 activation and synaptic loss in the hippocampus.

Discussion

C1-INH blocks the C1r/C1s proteases of the classical and lectin pathways to regulate activation of C3, and is FDA approved to treat hereditary angioedema in humans [43, 52]. Because we found increases in hippocampal protein levels of C1q and C3 that paralleled the development of learning and memory deficits in a rat model of SE and acquired epilepsy [27], we investigated if acute C1-INH treatment after SE had protective effects against hippocampal-dependent cognitive decline. We selected acute treatment at 4-48 hours after SE because during this period inflammatory cytokines peaked [31] and acute treatment with other immunosuppressants have been effective at promoting neuroprotection in models of acquired epilepsy [55]. While the C1-INH treatment given acutely after an episode of pilocarpine-induced SE showed positive effects in facilitating a faster recovery of the weight loss in SE animals (Figure 2) and promoting anxiolytic effects (Figure 3), it did not attenuate the development of hippocampal-dependent learning and memory deficits that occurred 2-3 weeks after SE (Figures 4–5). Interestingly and unexpectedly, we also found that acute C1-INH treatment exacerbated SE-induced microgliosis in the hippocampus at 3 days after SE (Fig. 6) and loss of synaptic proteins at 14 days after SE (Fig. 7).

The positive effects of C1-INH on weight recovery reported in this study (Figure 2) are consistent with other outcomes resulting from complement inhibition in experimental models of brain injury [23, 30]. C1-INH attenuated brain injury and cognitive deficits in experimental mouse models of TBI, ischemia, and stroke [30, 42, 56]. Mice treated with C1-INH immediately following controlled cortical impact TBI showed improved hippocampal-dependent spatial learning and memory, and a faster recovery of neurologic motor function compared to vehicle-treated injured mice [23, 29]. In addition, a single C1-INH injection within 5 to 6 hours after middle cerebral artery occlusion or ischemia-reperfusion in mice resulted in reduced size of ischemic volume, reduced mortality, and improved neurological outcomes [30, 42].

SE results in robust neuroimmune responses [57, 58] as well as transient, yet severe, weight loss [33]. In a model of organophosphorus compound-induced SE, treatment with an inhibitor of oxidative stress accelerated the rate of weight gain following a sharp decrease immediately after SE [33]. In addition, blocking circulating monocytes after SE also results in neuroprotection and accelerated weight gain [59]. These studies suggest that modulating immune signaling pathways can be beneficial for weight gain after SE. Together with our current findings with C1-INH treatment, these data suggest that the effects on weight recovery are long-lasting.

In this study we replicated previous findings that SE provokes hippocampal-dependent memory deficits in tests such as NOR and BM [12, 13, 27, 60]. Because increased classical complement pathway activation is linked to deficits in spatial memory, cognitive flexibility (reversal learning), recognition memory (NOR), and age-dependent memory decline in rodent models of neurodegeneration [25, 61], we expected that acute treatment [40] with the complement inhibitor C1-INH immediately after SE would prevent the associated learning and memory deficits. However, early C1-INH administration after SE did not alter SE-induced learning or memory deficits seen in NOR or BM (Figures 4–5). This may be due to differences in route of drug administration, dose, or time window of treatment. In other injury models, single C1-INH doses (15–20 U/kg) were administered intravenously between 5 and 90 minutes after onset of injury, similarly to the time points of drug administration in the present study [30, 42]. Here we administered C1-INH subcutaneously which also has been shown to be effective [62, 63]. The half-life of human-derived C1-INH is approximately 20 hours in human plasma and 4.5 hours in rats [64]. Despite this lower half-life in rats, C1-INH treatment in rats can have long-lasting positive results [42]. As for the time window of treatment, increased complement activation in the ischemia model occurs within hours of injury and appears to persist for weeks [24, 65], whereas maximal increases in C3 signaling occurs between 2-5 weeks after SE [27]. Therefore, adjusting the timeline of treatment may potentially be effective to attenuating the SE-induced cognitive decline. Alternative possibilities include that C1-INH treatment in SE rats may have anxiolytic effects thereby making the rats less sensitive to the BM anxiogenic stimulus (bright lights) and decreasing their desire to enter the dark escape box. This idea that is supported by the observation that SE+C1-INH rats spent less time in the outer part of the OF (Figure 3H) suggesting a decrease in anxiety-like behaviors. Future studies with C1-INH in normal (non-SE) rats may help further elucidate the effects of this drug and its mechanisms in the modulation of cognitive and anxiety behaviors.

Although C1-INH is a well-known modulator of the complement cascade [53], it is also associated with the activation of the kallikrein-kinin system (KKS) [66]. KKS plays a role in the regulation of inflammation, vascular permeability and blood pressure through signaling by the bradykinin peptide [67]. Farfara et al. (2019) recently showed that knocking down C1-INH in mice resulted in an increased activation of the bradykinin pathway that was coupled to microgliosis, astrogliosis, and neuroinflammation as well as with learning and memory deficits in the fear conditioning test [66]. Thus, it is possible that the exacerbated microgliosis seen in the SE+C1-INH group at 3 days (Figure 6A) may be the result of an unexpected activation of the KKS system. The increased microgliosis provoked by C1-INH in SE rats (Figure 6A) may have subsequently accelerated or exacerbated epileptogenic processes such as the increased C3 activation and the loss of synaptic proteins in the hippocampus we found at 14 days after SE (Figure 7). Note that similar to Farfara et al. (2019), we did not see changes in the levels of C3 protein immediately after treatment; though their study suppressed C1-INH for weeks. Moreover, these findings also suggest the possibility that the aggravated synaptic pathology in the hippocampus may have further impaired the memory acquisition of C1-INH rats in the NOR and BM tests (Figures 4 and 5).

Conclusions

This study demonstrated that C1-INH treatment early after SE may have some protective, albeit limited, effects on the physiological recovery of rats' weight and some anxiolytic effects. In parallel, this acute treatment did not significantly alter the SE-induced cognitive decline that occurs 2-3 weeks later in this rat model of SE and acquired TLE. Instead, acute C1-INH treatment immediately after SE may have exacerbated epileptogenic processes through enhancing microgliosis early after SE as well as C3 activation and synaptic loss at later time points. Further investigation is required to understand the effects of C1-INH on SE-induced neuronal injury, behavioral deficits, and seizure severity when given at later time points after SE or in epileptic animals.

Acknowledgments

List of Abbreviations:

SE	Status epilepticus
TLE	temporal lobe epilepsy
C1-INH	C1 esterase inhibitor
AD	Alzheimer's disease
TBI	traumatic brain injury
OF	Open Field

NOR	Novel Object Recognition
RI	Recognition Index
DI	Discrimination Index
BM	Barnes Maze
IR	ischemia-reperfusion

References

1. Thijs RD, et al., Epilepsy in adults. The Lancet, 2019 393(10172): p. 689–701.

2. Scharfman HE, The neurobiology of epilepsy. Curr Neurol Neurosci Rep, 2007 7(4): p. 348–54. [PubMed: 17618543]

3. Keezer MR, Sisodiya SM, and Sander JW, Comorbidities of epilepsy: current concepts and future perspectives. The Lancet Neurology, 2016 15(1): p. 106–115. [PubMed: 26549780]

4. Stafstrom CE, Epilepsy comorbidities: how can animal models help? Adv Exp Med Biol, 2014 813: p. 273–81. [PubMed: 25012384]

5. LaFrance WC, Kanner AM, and Hermann B, Chapter 20 Psychiatric Comorbidities in Epilepsy, in International Review of Neurobiology. 2008, Academic Press, p. 347–383.

6. Pichler M and Hocker S, Chapter 9 - Management of status epilepticus, in Handbook of Clinical Neurology, Wijdicks EFM and Kramer AH, Editors. 2017, Elsevier, p. 131–151.

7. Santamarina E, et al., Prognosis of status epilepticus (SE): Relationship between SE duration and subsequent development of epilepsy. Epilepsy Behav, 2015 49: p. 138–40. [PubMed: 26117525]

8. Meisenhelter S, Jobst BCJCN, and Reports N, Neurostimulation for Memory Enhancement in Epilepsy. 2018 18(6): p. 30.

9. McAuley JW, et al., Comparing patients' and practitioners' views on epilepsy concerns: A call to address memory concerns. Epilepsy & Behavior, 2010 19(4): p. 580–583. [PubMed: 20889386]

10. Breen EK, et al., Accelerated forgetting in patients with epilepsy: Evidence for an impairment in memory consolidation. Brain, 2000 123(3): p. 472–483. [PubMed: 10686171]

11. Schipper S, et al., Accelerated cognitive decline in a rodent model for temporal lobe epilepsy. Epilepsy & Behavior, 2016 65: p. 33–41. [PubMed: 27865173]

12. Pearson JN, Schulz KM, and Patel M, Specific alterations in the performance of learning and memory tasks in models of chemoconvulsant-induced status epilepticus. Epilepsy Reseach, 2014 108(6): p. 1032–1040.

13. Brewster AL, et al., Rapamycin reverses status epilepticus-induced memory deficits and dendritic damage. PLoS One, 2013 8(3): p. e57808. [PubMed: 23536771]

14. Oliveira C.V.d., et al., Evaluation of potential gender-related differences in behavioral and cognitive alterations following pilocarpine-induced status epilepticus in C57BL/6 mice. Physiology & Behavior, 2015 143: p. 142–150. [PubMed: 25749198]

15. Cho K-O, et al., Aberrant hippocampal neurogenesis contributes to epilepsy and associated cognitive decline. Nature Communications, 2015 6: p. 6606.

16. Sarma JV and Ward PA, The complement system. Cell Tissue Res, 2011 343(1): p. 227–35. [PubMed: 20838815]

17. Stephan AH, Barres BA, and Stevens B, The complement system: an unexpected role in synaptic pruning during development and disease. Annu Rev Neurosci, 2012 35: p. 369–89. [PubMed: 22715882]

18. Mortensen SA, et al., Structure and activation of C1, the complex initiating the classical pathway of the complement cascade. Proceedings of the National Academy of Sciences, 2017 114(5): p. 986–991.

19. Schafer DP, et al., Microglia sculpt postnatal neural circuits in an activity and complement-dependent manner. Neuron, 2012 74(4): p. 691–705. [PubMed: 22632727]

20. Stevens B, et al., The classical complement cascade mediates CNS synapse elimination. Cell, 2007 131(6): p. 1164–78. [PubMed: 18083105]

21. Presumey J, Bialas AR, and Carroll MC, Chapter Two - Complement System in Neural Synapse Elimination in Development and Disease, in Advances in Immunology, Alt FW, Editor. 2017, Academic Press p. 53–79.

22. Hong S, et al., Complement and microglia mediate early synapse loss in Alzheimer mouse models. Science, 2016 352: p. 712–716. [PubMed: 27033548]

23. Longhi L, et al. Neuroprotective effect of C1-inhibitor following traumatic brain injury in mice. 2008 Vienna: Springer Vienna.

24. Silverman SM, et al., C1q propagates microglial activation and neurodegeneration in the visual axis following retinal ischemia/reperfusion injury. Molecular Neurodegeneration, 2016 11(1): p. 1–16. [PubMed: 26758690]

25. Shi Q, et al., Complement C3-Deficient Mice Fail to Display Age-Related Hippocampal Decline. The Journal of Neuroscience, 2015 35(38): p. 13029–13042. [PubMed: 26400934]

26. Wyatt SK, et al., Enhanced classical complement pathway activation and altered phagocytosis signaling molecules in human epilepsy. Exp Neurol, 2017 295: p. 184–193. [PubMed: 28601603]

27. Schartz ND, et al., Status epilepticus triggers long-lasting activation of complement C1q-C3 signaling in the hippocampus that correlates with seizure frequency in experimental epilepsy. Neurobiol Dis, 2018 109(Pt A): p. 163–173. [PubMed: 29074125]

28. Davis AE, Lu F, and Mejia P, C1 inhibitor, a multi-functional serine protease inhibitor. Thromb Haemost, 2010 104(11): p. 886–893. [PubMed: 20806108]

29. Longhi L, et al., C1-inhibitor attenuates neurobehavioral deficits and reduces contusion volume after controlled cortical impact brain injury in mice*. Critical Care Medicine, 2009 37(2): p. 659–665. [PubMed: 19114897]

30. De Simoni MG, et al., Neuroprotection by complement (C1) inhibitor in mouse transient brain ischemia. J Cereb Blood Flow Metab, 2003 23(2): p. 232–9. [PubMed: 12571454]

31. Schartz ND, et al., Spatiotemporal profile of Map2 and microglial changes in the hippocampal CA1 region following pilocarpine-induced status epilepticus. Sci Rep, 2016 6: p. 24988. [PubMed: 27143585]

32. Racine RJ, Modification of seizure activity by electrical stimulation. II. Motor seizure. Electroencephalogr Clin Neurophysiol, 1972 32(3): p. 281–94. [PubMed: 4110397]

33. Rojas A, et al., Inhibition of the prostaglandin EP2 receptor is neuroprotective and accelerates functional recovery in a rat model of organophosphorus induced status epilepticus. Neuropharmacology, 2015 93: p. 15–27. [PubMed: 25656476]

34. Reynolds CD, et al., Oral aniracetam treatment in C57BL/6J mice without pre-existing cognitive dysfunction reveals no changes in learning, memory, anxiety or stereotypy. F1000Res, 2017 6: p. 1452. [PubMed: 29946420]

35. Bui AD, et al., Dentate gyrus mossy cells control spontaneous convulsive seizures and spatial memory. Science, 2018 359(6377): p. 787–790. [PubMed: 29449490]

36. Brewster AL, et al., Quantitative analysis and subcellular distribution of mRNA and protein expression of the hyperpolarization-activated cyclic nucleotide-gated channels throughout development in rat hippocampus. Cereb Cortex, 2007 17(3): p. 702–12. [PubMed: 16648453]

37. Cole TJ, Too many digits: the presentation of numerical data. Archives of disease in childhood, 2015 100(7): p. 608–609. [PubMed: 25877157]

38. Caliezi C, et al., C1-Esterase Inhibitor: An Anti-Inflammatory Agent and Its Potential Use in the Treatment of Diseases Other Than Hereditary Angioedema. Pharmacological Reviews, 2000 52(1): p. 91–112. [PubMed: 10699156]

39. Aronica E, et al., Complement activation in experimental and human temporal lobe epilepsy. Neurobiol Dis, 2007 26(3): p. 497–511. [PubMed: 17412602]

40. Benson MJ, et al., A novel anticonvulsant mechanism via inhibition of complement receptor C5ar1 in murine epilepsy models. Neurobiol Dis, 2015 76: p. 87–97. [PubMed: 25681535]

41. Kharatishvili I, et al., MRI changes and complement activation correlate with epileptogenicity in a mouse model of temporal lobe epilepsy. Brain Struct Funct, 2014 219(2): p. 683–706. [PubMed: 23474541]

42. Heydenreich N, et al., C1-inhibitor protects from brain ischemia-reperfusion injury by combined antiinflammatory and antithrombotic mechanisms. Stroke, 2012 43(9): p. 2457–67. [PubMed: 22744646]

43. Mollnes TE and Kirschfink M, Strategies of therapeutic complement inhibition. Mol Immunol, 2006 43(1-2): p. 107–21. [PubMed: 16011851]

44. Wyatt-Johnson SK, Herr SA, and Brewster AL, Status Epilepticus Triggers Time-Dependent Alterations in Microglia Abundance and Morphological Phenotypes in the Hippocampus. Front Neurol, 2017 8: p. 700. [PubMed: 29326654]

45. Swann JW and Hablitz JJ, Cellular abnormalities and synaptic plasticity in seizure disorders of the immature nervous system. Ment Retard Dev Disabil Res Rev, 2000 6(4): p. 258–67. [PubMed: 11107191]

46. Holmes GL, Effects of early seizures on later behavior and epileptogenicity. Ment Retard Dev Disabil Res Rev, 2004 10(2): p. 101–5. [PubMed: 15362164]

47. Wong M, Modulation of dendritic spines in epilepsy: cellular mechanisms and functional implications. Epilepsy Behav, 2005 7(4): p. 569–77. [PubMed: 16246628]

48. Nolan MA, et al., Intelligence in childhood epilepsy syndromes. Epilepsy Res, 2003 53(1-2): p. 139–50. [PubMed: 12576175]

49. Chauviere L, et al., Early deficits in spatial memory and theta rhythm in experimental temporal lobe epilepsy. J Neurosci, 2009 29(17): p. 5402–10. [PubMed: 19403808]

50. Jacobs MP, et al., Curing epilepsy: progress and future directions. Epilepsy Behav, 2009 14(3): p. 438–45. [PubMed: 19341977]

51. Becker AJ, Review: Animal models of acquired epilepsy: insights into mechanisms of human epileptogenesis. Neuropathology and Applied Neurobiology, 2018 44(1): p. 112–129. [PubMed: 29130506]

52. Sahu A and Lambris JD, Complement inhibitors: a resurgent concept in anti-inflammatory therapeutics. Immunopharmacology, 2000 49(1-2): p. 133–48. [PubMed: 10904113]

53. Barnum SR, Complement: A primer for the coming therapeutic revolution. Pharmacol Ther, 2017 172: p. 63–72. [PubMed: 27914981]

54. Vasek MJ, et al., A complement-microglial axis drives synapse loss during virus-induced memory impairment. Nature, 2016 534(7608): p. 538–43. [PubMed: 27337340]

55. Guo D, et al., Rapamycin prevents acute dendritic injury following seizures. Annals of Clinical and Translational Neurology, 2016 3(3): p. 180–190. [PubMed: 27042678]

56. De Simoni MG, et al., The Powerful Neuroprotective Action of C1-Inhibitor on Brain Ischemia-Reperfusion Injury Does Not Require C1q. The American Journal of Pathology, 2004 164(5): p. 1857–1863. [PubMed: 15111332]

57. Vezzani A, Friedman A, and Dingledine RJ, The role of inflammation in epileptogenesis. Neuropharmacology, 2013 69: p. 16–24. [PubMed: 22521336]

58. Vezzani A, et al., The role of inflammation in epilepsy. Nat Rev Neurol, 2011 7(1): p. 31–40. [PubMed: 21135885]

59. Varvel NH, et al., Infiltrating monocytes promote brain inflammation and exacerbate neuronal damage after status epilepticus. Proceedings of the National Academy of Sciences, 2016 113(38): p. E5665–E5674.

60. Levin JR, Serrano G, and Dingledine R, Reduction in delayed mortality and subtle improvement in retrograde memory performance in pilocarpine-treated mice with conditional neuronal deletion of cyclooxygenase-2 gene. Epilepsia, 2012 53(8): p. 1411–1420. [PubMed: 22780884]

61. Hernandez MX, et al., Prevention of C5aR1 signaling delays microglial inflammatory polarization, favors clearance pathways and suppresses cognitive loss. Molecular Neurodegeneration, 2017 12(1): p. 66. [PubMed: 28923083]

62. Martinez-Saguer I, et al., Pharmacokinetics of plasma-derived C1-esterase inhibitor after subcutaneous versus intravenous administration in subjects with mild or moderate hereditary angioedema: the PASSION study. Transfusion, 2014 54(6): p. 1552–1561. [PubMed: 24266596]

63. Emmens RW, et al., Evaluating the efficacy of subcutaneous C1-esterase inhibitor administration for use in rat models of inflammatory diseases. Drug Deliv, 2013.

64. de Smet BJ, et al., Clearance of human native, proteinase-complexed, and proteolytically inactivated C1-inhibitor in rats. Blood, 1993 81(1): p. 56–61. [PubMed: 8417802]

65. Väkevä A, et al., Time course of complement activation and inhibitor expression after ischemic injury of rat myocardium. The American Journal of Pathology, 1994 144(6): p. 1357–1368. [PubMed: 7515561]

66. Farfara D, et al., Knockdown of circulating C1 inhibitor induces neurovascular impairment, glial cell activation, neuroinflammation, and behavioral deficits. Glia, 2019 67(7): p. 1359–1373. [PubMed: 30882931]

67. Nokkari A, et al., Implication of the Kallikrein-Kinin system in neurological disorders: Quest for potential biomarkers and mechanisms. Prog Neurobiol, 2018 165-167: p. 26–50. [PubMed: 29355711]

Highlights

- Status epilepticus (SE) results in complement hyperactivation and memory deficits

- C1 esterase inhibitor (C1-INH) accelerates weight recovery following SE

- C1-INH does not attenuate SE-induced memory deficits

- SE-induced increases in C3 are inversely correlated to loss of synaptic proteins
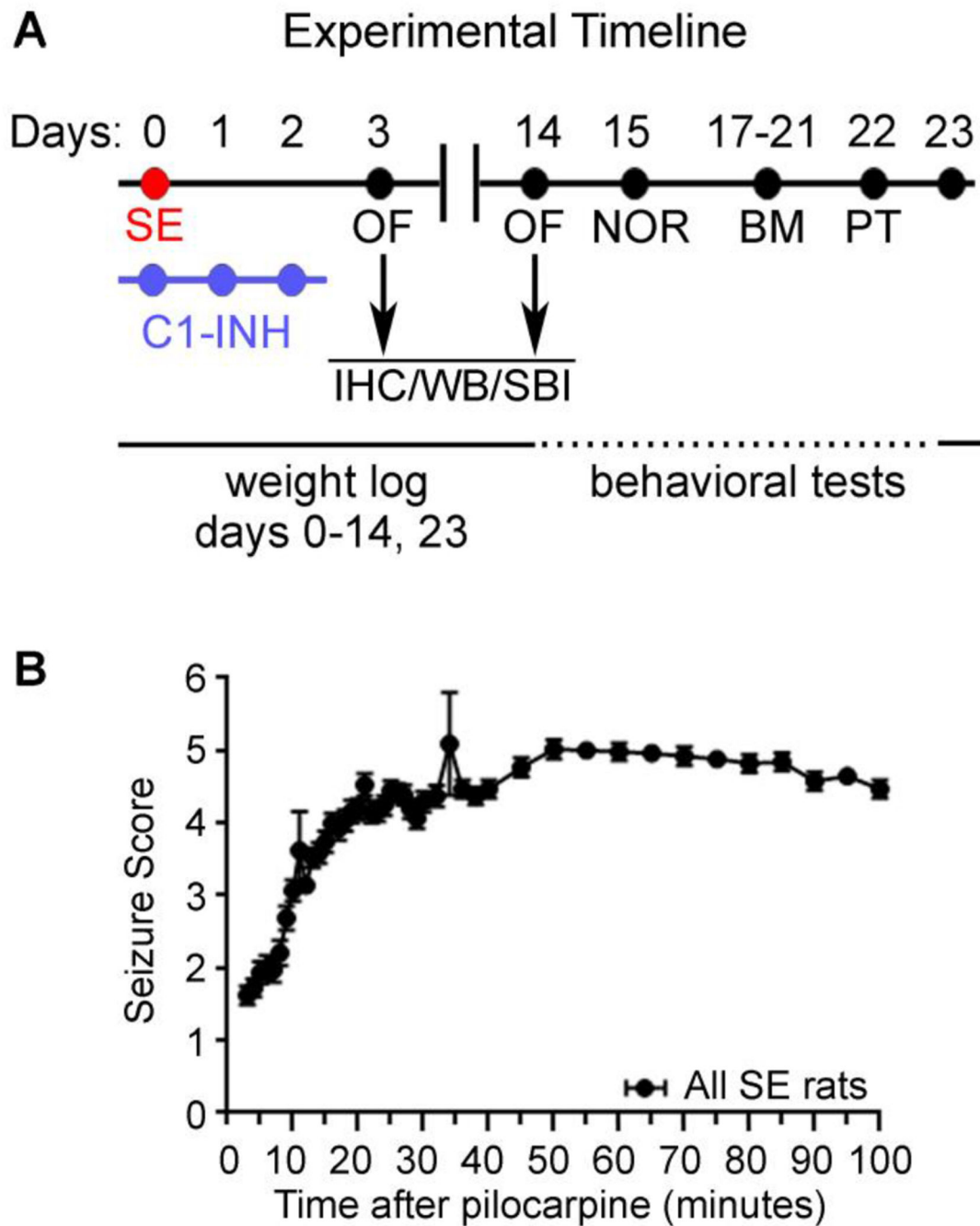
Figure 1.
Experimental design and induction of status epilepticus (SE). (**A**) Timeline of the experimental design. Following pilocarpine-induced SE induction (day 0) and C1 esterase inhibitor (C1-INH) treatment (20 Units/kg (i.p.) on days 0, 1, and 2) rats were subjected to a battery of behavioral tests (days 3-22) including Open Field (OF), Novel Object Recognition (NOR), Barnes Maze (BM) and Probe trial (PT). Brain samples were collected at 3 and 14 days after SE for immunohistochemistry (IHC), Western blotting (WB), or solid-based immunoassay (SBI). Rats' weights were recorded daily from day 0-14 and on day.

Behavioral seizures were monitored for up to two hours after pilocarpine injection. All rats included in the study reached SE score of at least 4.5.
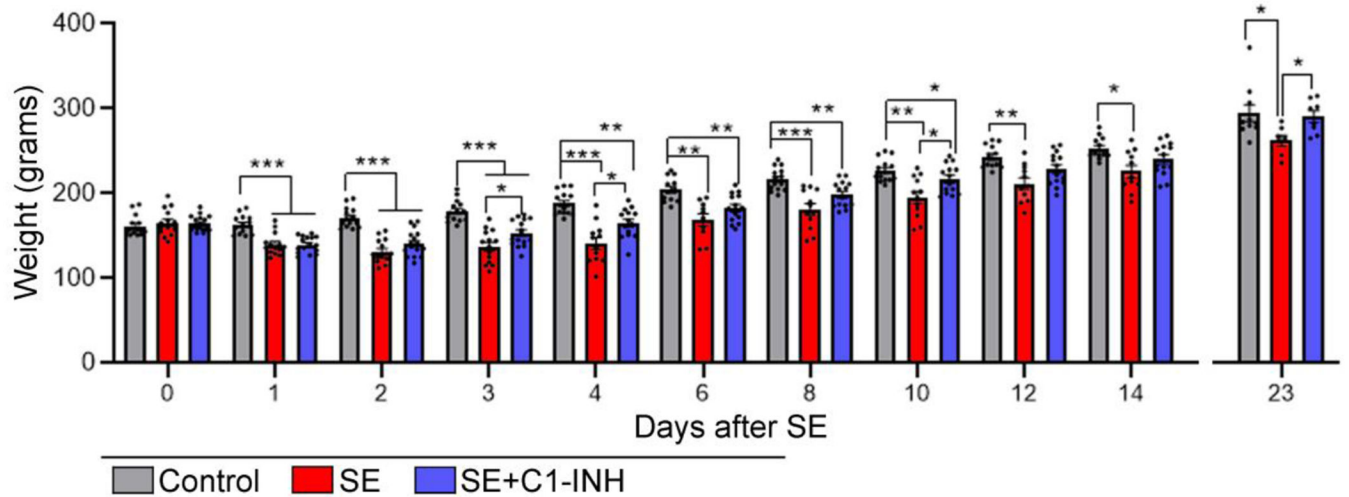
Figure 2.
Acute C1 esterase inhibitor (C1-INH) treatment after status epilepticus (SE) promotes weight gain. Graphs show weight comparisons of control, SE, and SE+C1-INH rats at experimental days 0-14 and 23. Data are shown as mean +/− standard error of the mean. *, p < 0.05; **, p < 0.01; ***, p < 0.001 by repeated measures ANOVA with Tukey's post hoc test. Controls, N=10-14; SE, N=7-14; SE+C1-INH, N=8-16.
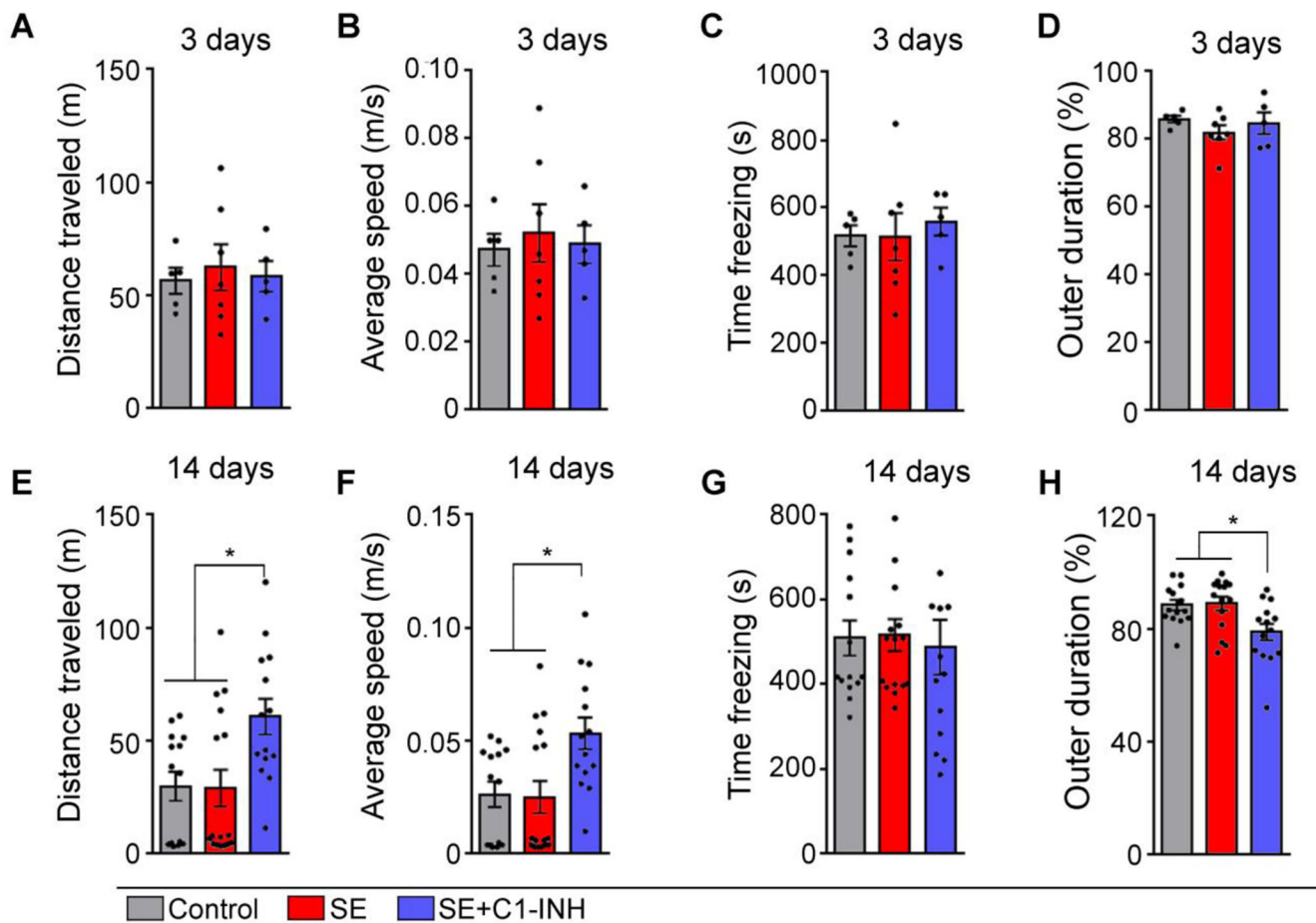
Figure 3.
Effects of acute C1 esterase inhibitor (C1-INH) treatment after status epilepticus (SE) on open field (OF) outcomes. The OF test was performed at 3 (**A-D**) and 14 days (**E-H**) after SE in control, SE, and SE+C1-INH rats. Distance traveled (**A, E**) and average speed (**B, F**) measured locomotion. Time freezing (**C** and **G**) and time spent in outer portion of the OF chamber (outer duration) (**D, H**) measured anxiety-like behaviors. Data are shown as mean +/− standard error of the mean. *, $p < 0.05$ by one-way ANOVA with Tukey's post hoc test. Controls, N=14; SE, N=16; SE+C1-INH, N=14.
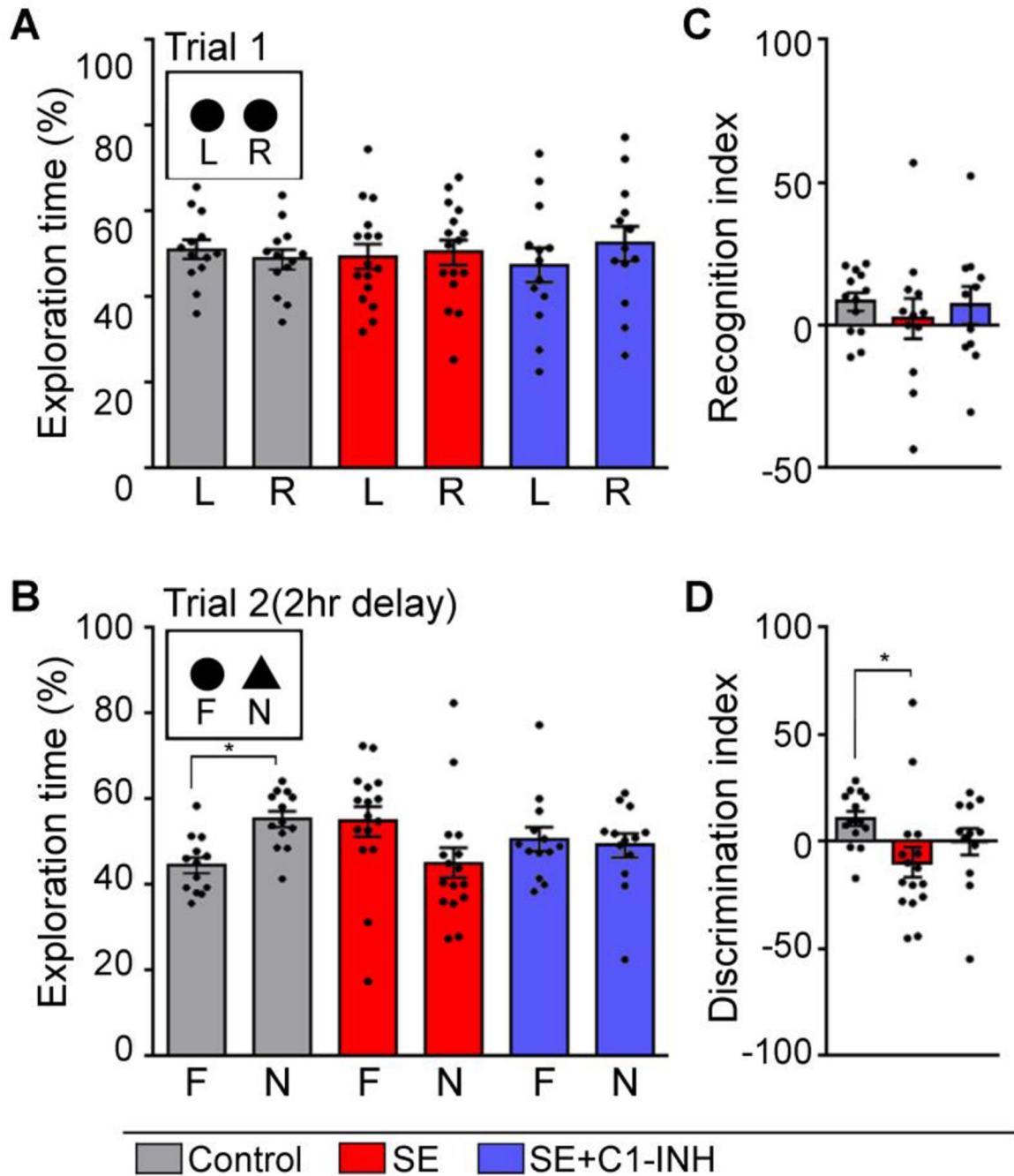
Figure 4.
Acute C1 esterase inhibitor (C1-INH) treatment after status epilepticus (SE) does not attenuate deficits in recognition memory determined with the novel object recognition (NOR) test. The NOR test was performed at 14-15 days after SE in control, SE, SE+C1-INH rats. (**A**) Graphs show the percent exploration time of two similar objects, left (L) and right (R), during trial 1. (**B**) Graphs show the percent exploration of the familiar (F) and novel (N) objects during trial 2. (**C**) Recognition index shows the difference in exploration time of the familiar object between NOR trials 1 and 2 [(F1-F2)/(F1+F2)]. (**D**) Discrimination index

shows the difference in exploration time between the familiar and novel objects during NOR trial 2 [(N-F)/(N+F)]. Data are shown as mean +/− standard error of the mean. *, p < 0.05 by paired t-test (**A, B**) and one-way ANOVA with Tukey's post hoc test (**C, D**). Controls, N=13; SE, N=16; SE+C1-INH, N=13.
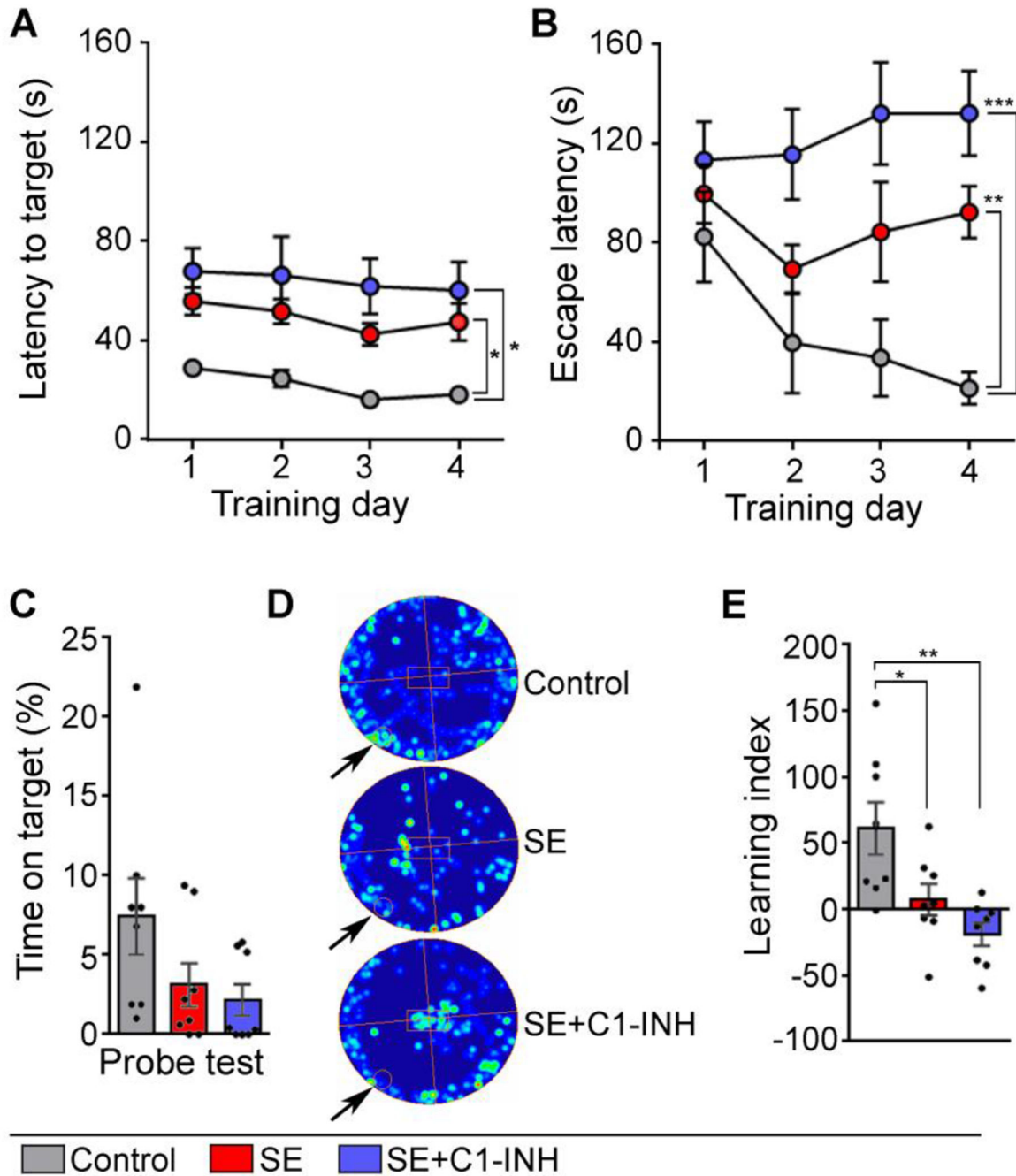
Figure 5.
Acute C1 esterase inhibitor (C1-INH) treatment after status epilepticus (SE) does not attenuate deficits in hippocampal-dependent spatial learning and memory determined with the Barnes Maze (BM). BM was performed on days 17-21 after SE in control, SE, SE+C1-INH rats. (**A-B**) The graph shows the time to first reach (**A**) and to enter (**B**) the escape box on the BM platform (escape latency) during the training period (BM days 1-4; 4 trials/day). (**C**) The probe trial shows the percent of time spent over the covered escape box (target hole) (BM day 5). (**D**) Shows representative heat maps of rats' movements during the probe trial

for a control, SE, and SE+C1-INH rat (arrow points to the location of the target hole with escape box). (**E**) Learning index shows the difference in the escape latency between training days 1 and 4. Data are shown as mean +/− standard error of the mean. *, $p < 0.05$; **, $p < 0.01$; ***, $p < 0.001$ by repeated measures ANOVA with Tukey's post hoc test. Controls, N=8; SE, N=8; SE+C1-INH, N=8.
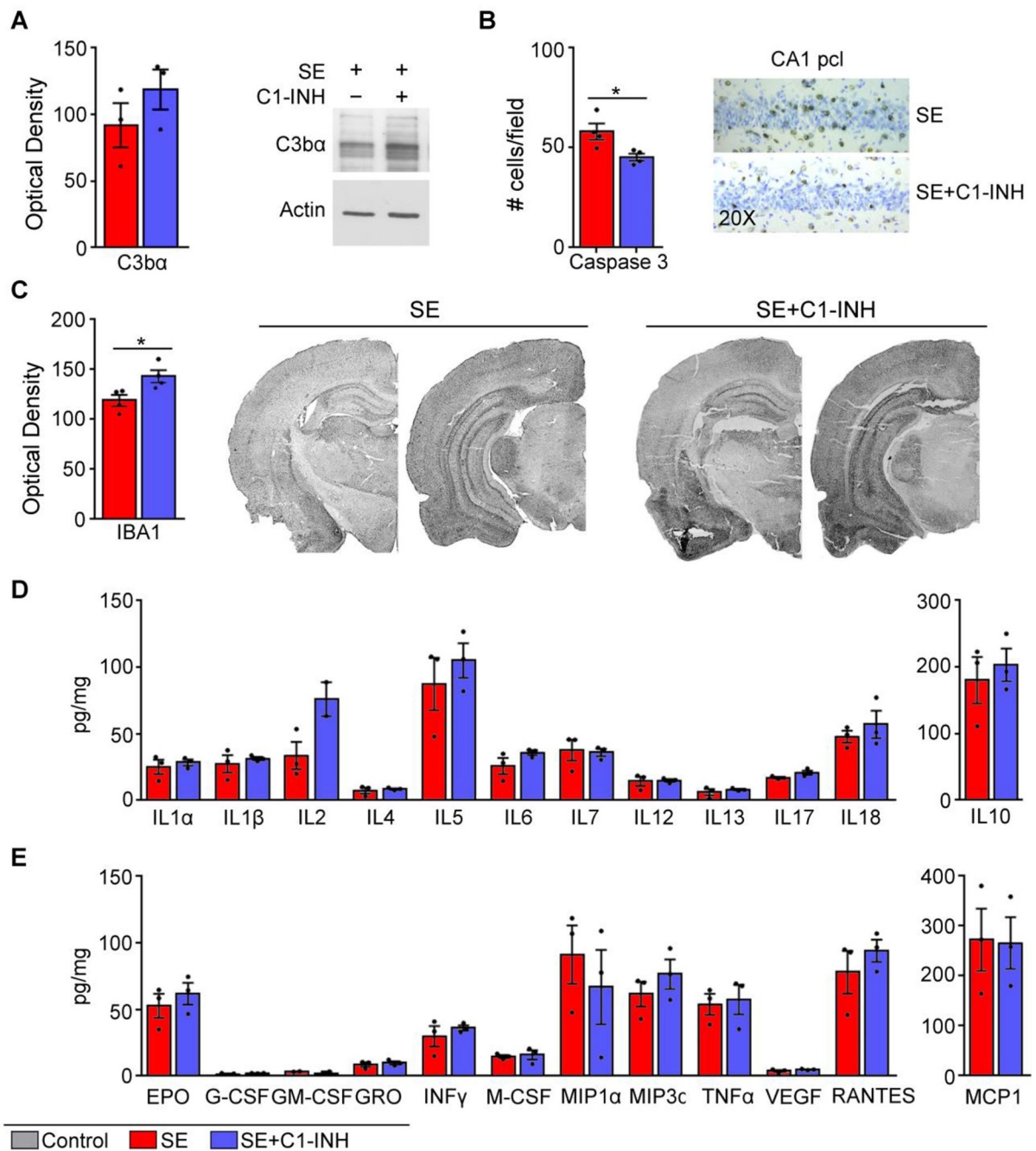
Figure 6.
Acute C1 esterase inhibitor (C1-INH) treatment after status epilepticus (SE) promotes microgliosis at 3 days after SE. (**A**) Quantification of immunoreactive bands for C3bα and actin was done in hippocampal homogenates derived from SE and SE+C1-INH rats (N=3/group). C3bα was normalized to actin. (**B**) Quantification of caspase-3 positive cells shown next to representative images of caspase-3 staining in the CA1 pyramidal cell layer in SE +veh and SE+C1-INH hippocampi (N=4/group). (**C**) Quantification of IBA1 signal intensity in hippocampus is shown along representative images of IBA1-stained microglia from dorsal
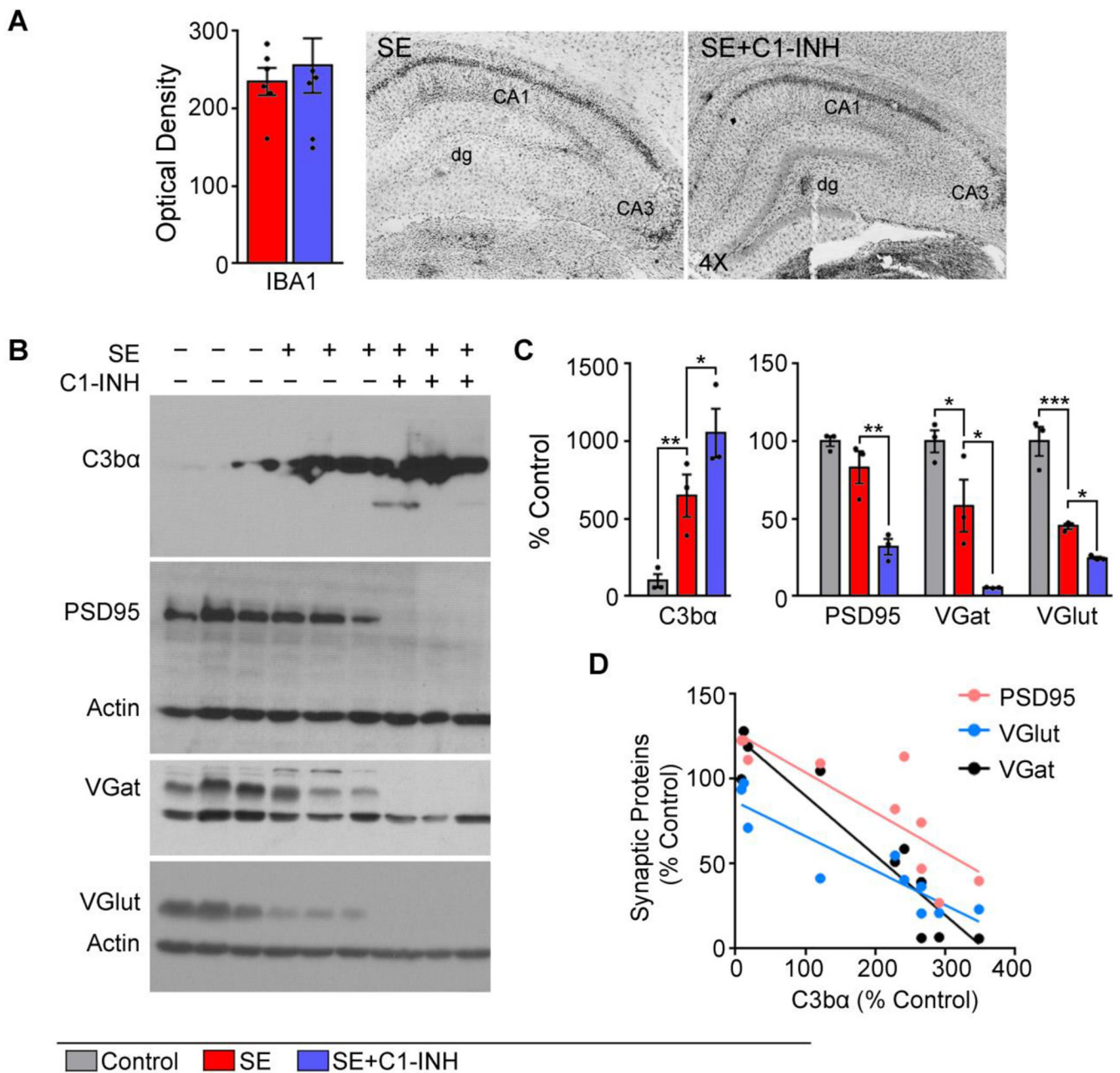
and ventral brain sections from SE and SE+C1-INH rats (N=4/group). (**D-E**) Solid-based immunoassay showed no alterations in 24 different inflammatory molecules. Data are shown as mean +/− standard error of the mean. *, $p < 0.05$ by independent t-test.

Figure 7.
Acute C1 esterase inhibitor (C1-INH) treatment after status epilepticus (SE) exacerbates C3 activation and synaptic protein loss at 14 days after SE. (**A**) Quantification of IBA1 signal intensity is shown along representative images of IBA1-stained microglia in hippocampi from SE and SE+C1-INH rats (N=5/group). (**B-C**) Quantification of immunoreactive bands for C3bα, PSD95, VGlut, VGat, and actin was done in hippocampal homogenates derived from control, SE, or SE+C1-INH rats (N=3/group). All immunoreactive bands were normalized to actin. (**D**) Density data for C3 plotted against that of synaptic proteins show

an inverse correlation. Data are shown as mean +/− standard error of the mean. *, $p < 0.05$; **, $p < 0.01$, ***, $p < 0,001$ by independent t-test or ANOVA with Tukey's post hoc test.